

See discussions, stats, and author profiles for this publication at: <https://www.researchgate.net/publication/228061452>

Design, synthesis and biological activity of 6-substituted carbamoyl benzimidazoles as new nonpeptidic angiotensin II AT(1) receptor antagonists

ARTICLE in BIOORGANIC & MEDICINAL CHEMISTRY · JUNE 2012

Impact Factor: 2.79 · DOI: 10.1016/j.bmc.2012.05.056 · Source: PubMed

CITATIONS

10

READS

38

11 AUTHORS, INCLUDING:



Jin-Liang Wang

Beijing Institute of Technology

6 PUBLICATIONS 61 CITATIONS

SEE PROFILE



Di Xu

Peking University

16 PUBLICATIONS 94 CITATIONS

SEE PROFILE



Fan Fei

The University of Manchester

7 PUBLICATIONS 53 CITATIONS

SEE PROFILE



Design, synthesis and biological activity of 6-substituted carbamoyl benzimidazoles as new nonpeptidic angiotensin II AT₁ receptor antagonists

Jun Zhang^a, Jin-Liang Wang^a, Zhi-Ming Zhou^{a,*}, Zhi-Huai Li^a, Wei-Zhe Xue^a, Di Xu^a, Li-Ping Hao^a, Xiao-Feng Han^a, Fan Fei^a, Ting Liu^b, Ai-Hua Liang^b

^a R&D Center for Pharmaceuticals, School of Chemical Engineering & the Environment, Beijing Institute of Technology, Beijing 100081, China

^b Institute of Chinese Materia Medica, China Academy of Chinese Medical Science, Beijing 100029, China

ARTICLE INFO

Article history:

Received 4 April 2012

Revised 28 May 2012

Accepted 29 May 2012

Available online 5 June 2012

Keywords:

Angiotensin II AT₁ receptor antagonists

carbamoyl benzimidazole

Hypertension

ABSTRACT

A series of 6-substituted carbamoyl benzimidazoles were designed and synthesised as new nonpeptidic angiotensin II AT₁ receptor antagonists. The preliminary pharmacological evaluation revealed a nanomolar AT₁ receptor binding affinity for all compounds in the series, and a potent antagonistic activity in an isolated rabbit aortic strip functional assay for compounds **6f**, **6g**, **6h** and **6k** was also demonstrated. Furthermore, evaluation in spontaneous hypertensive rats and a preliminary toxicity evaluation showed that compound **6g** is an orally active AT₁ receptor antagonist with low toxicity.

© 2012 Elsevier Ltd. All rights reserved.

1. Introduction

Antagonism of octapeptide angiotensin II (Ang II) at the AT₁ receptor offers real promise as a therapy for hypertension and heart failure,^{1,2} although the functional role of the AT₂ receptor has yet to be clearly demonstrated.³ The discovery of the AT₁-selective Ang II antagonist Losartan has stimulated extensive research on other nonpeptide Ang II antagonists bearing novel heterocyclic moieties.^{4,5} Among the large variety of the heterocyclic systems developed, the ortho-fused bicyclic moiety benzimidazole appears to be, from the point of view of the interaction with the AT₁ receptor, a particularly effective heterocyclic system.^{6,7} This compound is commercially available as Candesartan⁸ and is the most potent AT₁ antagonist so far. Meanwhile, modification of the benzimidazole nucleus also demonstrated that the presence of an acylureas lipophilic group at the 6-position,⁹ a carboxylic group at the 7-position,¹⁰ and a nitro group at the 5-position¹¹ were favourable for Ang II antagonism. However, benzimidazole-6 carboxylic acid derivatives have been scarcely exploited in treatments for hypertension and heart failure. The presence of the L3 lipophilic pockets proposed in the literature¹² suggested that a carboxamide with an alkyl-chain-bearing phenyl group may provide additional interactions (Van der Waals force, e.g., π - π) that consequently enhance

the overall interaction between the antagonist and the receptor. Interestingly, it has been shown in the literature¹³ that phenylethylamino can effectively lower hypertensive pressure. Therefore, N-substituted alkyl 1-[2'-(1H-tetrazol-5-yl)-1,1'-biphenyl-4-yl]-methyl-4-methyl-2-n-propyl-1H-benzimidazole-6-carboxamide compounds (Fig. 1) were designed with a carbamoyl group at the 6-position, which are expected to have higher activity than Losartan. A previous study in our laboratory^{14,15} regarding the electrostatic potential of the benzimidazole nucleus showed that an electron-donating group at the phenyl ring of the phenylethylamino fragment facilitates the activity. Therefore, in the present study, we designed, synthesised and evaluated 6-substituted carbamoyl benzimidazoles bearing methoxy on the phenyl side and the effect of the length of the bridge chain using Losartan as reference compound.

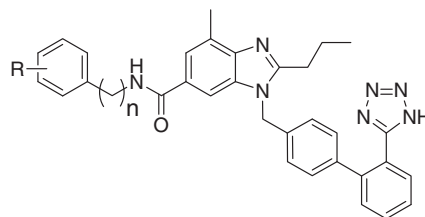
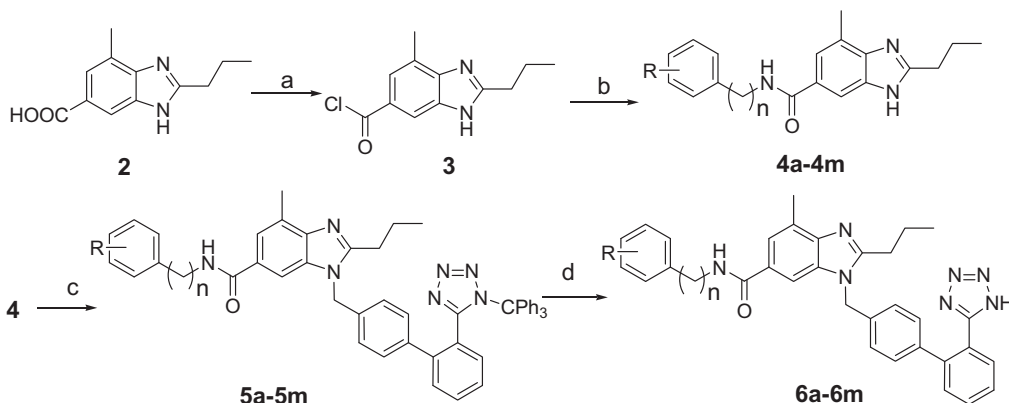


Figure 1. The structure of the designed compounds.

* Corresponding author. Tel./fax: +86 10 68918982.

E-mail address: zzm@bit.edu.cn (Z.-M. Zhou).



Scheme 1. Reagents and conditions: (a) thionyl dichloride, reflux, 3 h; (b) various substituted amines, Et₃N, DCM, rt, 6 h; (c) 5-(4'-bromomethyl-1,1'-biphenyl-2-yl)-1-triphenylmethyl-1H tetrazole, *t*-BuOK, DMF, rt, 12 h; (d) 10% HCl, THF, MeOH; NaOH; HCl, overnight.

2. Results and discussion

2.1. Chemistry

The target compounds **6a–6m** were synthesised according to the route described in Scheme 1, and the starting material 4-methyl-2-propyl-1H-benzimidazole-6-carboxylic acid (**2**) used in this scheme was prepared from 3-methyl-4-nitrobenzoic acid according to the reported methods.¹⁴ This compound was converted to the acyl chloride with thionyl dichloride under reflux conditions; the acyl chloride was then coupled with different amines to give the acylamide compounds **4a–4m** with an 82–90% yield. The acylamides were then alkylated with 5-(4'-bromomethyl-1,1'-biphenyl-2-yl)-1-triphenylmethyl-1H-tetrazole using potassium *tert*-butoxide in DMF to give the corresponding products in yields of 60–70%. The last step, deprotection of **5a–5m** using diluted hydrochloride acid followed by sodium hydroxide, was accomplished with a greater than 90% yield. All target compounds were identified by IR, ¹H NMR, ¹³C NMR and HRMS.

2.2. Biological evaluation

The prepared compounds were evaluated for their in vitro Ang II receptor binding affinity based on the competitive inhibition of [¹²⁵I] Ang II binding to the AT₁ receptors by a conventional ligand-binding assay as described previously.¹⁶ The results are expressed as IC₅₀ values, which is the concentration of a compound that inhibits [¹²⁵I] Ang II binding to the receptor by 50%. The antagonistic activity of the more potent compounds (**6f**, **6g**, **6h** and **6k**) were also investigated in vitro using the contractile response of isolated rabbit aortic strips in a functional assay.¹⁷ Losartan was taken as a positive control drug in the assays. At last, the most potent compound **6g** was evaluated in an in vivo model.

As summarised in Table 1, the binding assay and the antagonistic activity results showed that all compounds displayed a certain extent of inhibition activity, as expected. Most of the compounds showed high activities for the binding affinities in the submicromolar range. Of all the synthesised compounds, compound **6g** was the most potent compound (IC₅₀ = 0.9 nM), exhibiting almost the same binding affinity as the marketed AT₁ receptor antagonist telmisartan (IC₅₀ = 1.0, 0.33 nM¹⁸), and about 12-fold the affinity of losartan (IC₅₀ = 16.2, 150, 19 6.7 nM²⁰). The pA₂ 8.77 also shows that this compound contains more potent antagonist activity than the positive control losartan (pA₂ = 7.9). Compounds **6f** (IC₅₀ = 1.3 nM), **6h** (IC₅₀ = 2.6 nM) and **6k** (IC₅₀ = 3.7 nM) were also much more active than losartan. The pA₂ of compounds **6f** and **6k** are 8.32 and 8.74, respectively, which are also higher than that of losartan. In

addition, compounds **6a**, **6c**, **6e**, **6i**, **6j** and **6l** showed the same activity level as losartan (10 nM < AT₁ IC₅₀ < 100 nM). These results suggested that both the length of the aliphatic chains (which connect the acylamino moiety and the phenyl ring) and the substitution pattern on the aromatics played key roles in the binding affinity.

Based on the results of in vitro Ang II-binding assays and functional antagonism studies, **6g** was selected for further evaluation using in vivo models. When evaluated orally in conscious, spontaneously hypertensive rats (SHR), at doses of 10 mg/kg, compound **6g** significantly decreased blood pressure by more than 30 mmHg (Fig. 2), suggesting that it is more efficacious than losartan.

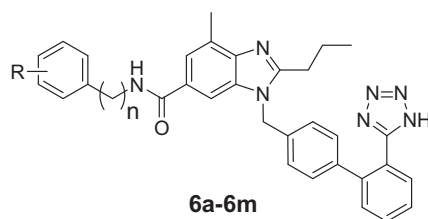
2.3. Molecular modelling

In the molecular modelling simulation study, six clinically used sartans (Fig. 3) were selected as the training set, and the pharmacophore hypothesis generation was performed using the HipHop module of the Discovery Studio software.²¹ Although the 3D structure of the AT₁ receptor is unknown, an ideal pharmacophore hypothesis can be identified.²² Accordingly, we used the method as a template representing the geometry of the receptor sites as a collection of functional groups in space. In this method, the fit value indicates how well the features in the pharmacophore map the chemical features in the molecule.²³ The higher the fit value, the more active a compound is. The fit values of the synthesised compounds were determined based on the hypothesis of AT₁ receptor antagonism using the best-fit algorithm as described in the literature.²⁴

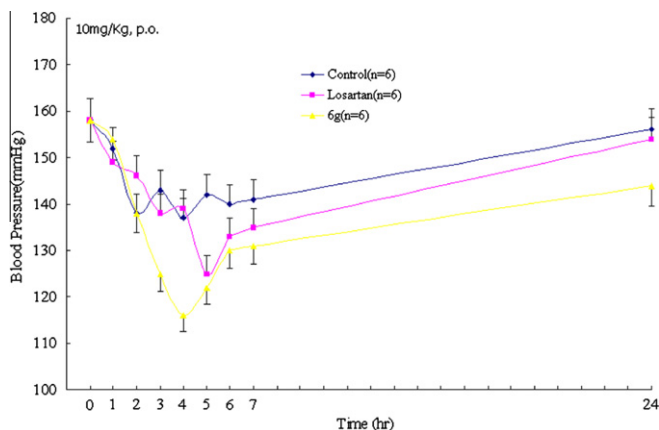
In this study, there are five features in the selected pharmacophore hypothesis, so the highest fit value is 5. Accordingly, the estimated activity could be classified according to the fit value as highly active (fit value >4, +++), moderately active (2 < fit value <4, ++), and low activity (fit value <4, +). All synthesised compounds in this study were also classified according to the literature²³ by their activity as highly active (<100 nM, +++), moderately active (100–10000 nM, ++), and low activity (>10000 nM, +). All highly active compounds were predicted correctly, only three moderately active compounds were predicted to be highly active. The results showed that despite these disparities, the pharmacophore hypothesis is reasonable. Furthermore, the molecular modelling simulation performed above reflected the interaction of ligands with the AT₁ receptor. Unexpectedly, it was the benzene ring in the phenylethyl, rather than the propyl at the 2-position of the benzimidazole ring that mapped onto the hydrophobic aliphatic feature. The same binding modality was also observed in the mapping of telmisartan with the pharmacophore (Fig. 4), in which

Table 1

Fit values on the selected pharmacophore and experimental data of the target compounds



Compod No.	n	R	Fit value	LC ₅₀ (nM)	Est. act. scale ^b	Exp. act. scale ^c	pA ₂	LC ₅₀ (mg L ⁻¹)
6a	1	H	4.78	410	+++	++		64
6b	1	2-OMe	4.70	19.7	+++	+++		66
6c	1	3-OMe	4.77	78.3	+++	+++		>100 ^d
6d	1	4-OMe	4.87	118.5	+++	++		>100
6e	1	3,4-Di-OMe	4.90	96.8	+++	+++		>100
6f	2	H	4.90	1.3	+++	+++	8.32	>100
6g	2 ^a	H	4.84	0.9	+++	+++	8.77	>100
6h	2	3-OMe	4.81	2.6	+++	+++	7.83	>100
6i	2	4-OMe	4.85	22.5	+++	+++		>100
6j	2	2,5-Di-OMe	4.71	78	+++	+++		>100
6k	2	3,4-Di-OMe	4.91	3.7	+++	+++	8.74	>100
6l	2	2-F	4.82	37.6	+++	+++		17
6m	2	4-F	4.93	209	+++	++		60
		Losartan	4.76	16.2	+++	+++	7.90	210
		Telmisartan	4.91	1.0	+++	+++		>100

^a The group between the amide group and the phenyl group is 2-methylethyl.^b Estimated activity scale: highly active (fit value >4, +++), moderately active (2 < fit value <4, ++) and low activity (fit value <4, +).^c Activity scale: highly active (<100 nM, +++), moderately active (100–10,000 nM, ++) and low activity (>10,000 nM, +).²²^d No LC₅₀ value could be determined because this compound did not produce more than 50% inhibition of the luminescence of *P. phosphoreum* at the saturated concentration level.**Figure 2.** Effects of **6g** and losartan (10 mg/Kg po) on mean arterial pressure in conscious SHR after oral administration.

it was the methyl in the second benzimidazole ring and not the propyl that mapped onto the hydrophobic aliphatic feature. However, in the case of losartan, it was the alkyl substituent that mapped onto the hydrophobic aliphatic feature (Fig. 5). This difference implied that the interaction modality of **6g**, like that of telmisartan, was not exactly the same as that of losartan. It is worth noting that the different interaction modalities of telmisartan and losartan have been reported in the literature²⁵ and were obtained through the docking of ligands with the homology-modelled AT₁ receptor.

2.4. Toxicity assay

Furthermore, a preliminary evaluation of toxicity against luminescent bacteria was performed on the prepared compounds

according to the standard Microtox test using luminescent bacteria. This assay is considered to be a useful tool and provides quick and reliable data.²⁶

In the toxicity assay, the results of the Microtox test are expressed in terms of LC₅₀ values. LC₅₀ is the concentration in water that inhibits 50% of a test batch of *Photobacterium phosphoreum* as exemplified by compound **6l** and **6m** in Figure 6. The lower the LC₅₀ value, the greater the toxicity of the sample is.²⁷ The results revealed that the LC₅₀ values of most of our synthetic compounds and telmisartan are higher than 100 mg L⁻¹, as they did not produce more than 50% inhibition of bacterial luminescence at the saturated concentration level. It is worth mentioning that the LC₅₀ value of losartan is 331 mg L⁻¹, which is almost the same as that (210 mg L⁻¹) obtained in another paper when algae were used.²⁸ This method provided a choice to evaluate the preliminary toxicity of these compounds, and the results showed that the toxicity of most compounds of the compounds is as low as that of telmisartan.

3. Conclusions

In summary, a series of 6-substituted carbamoyl benzimidazoles were designed and synthesised as new nonpeptidic AT₁ receptor antagonists. Compound **6g** was found to be the most potent AT₁-selective AT₁ receptor antagonists with low toxicity, it could be used as lead compounds for the further design and synthesis of more potent nonpeptidic angiotensin II AT₁ receptor antagonists.

4. Experimental

4.1. Chemistry

The melting points were determined on an XT-4A melting point apparatus and are uncorrected. All the target compounds were

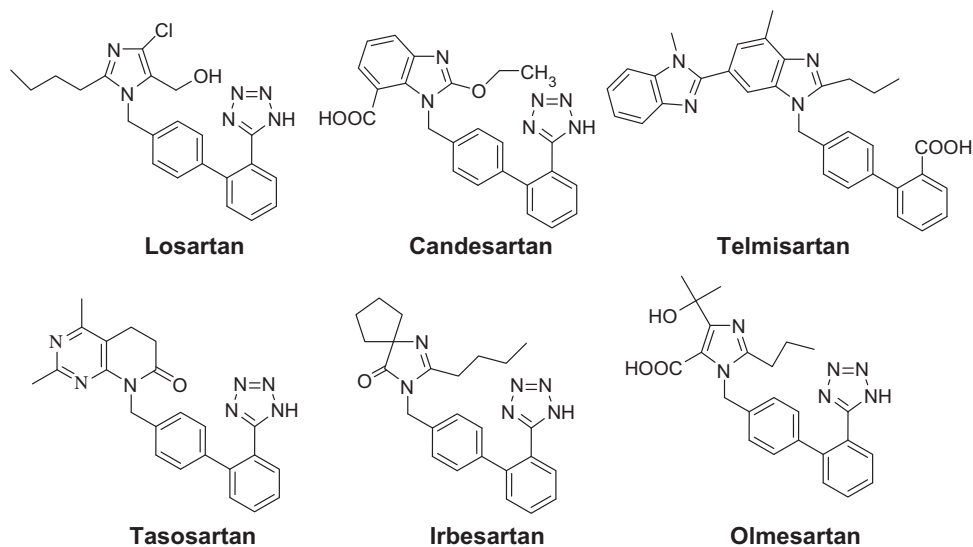


Figure 3. Structures of several AT₁ receptor antagonists.

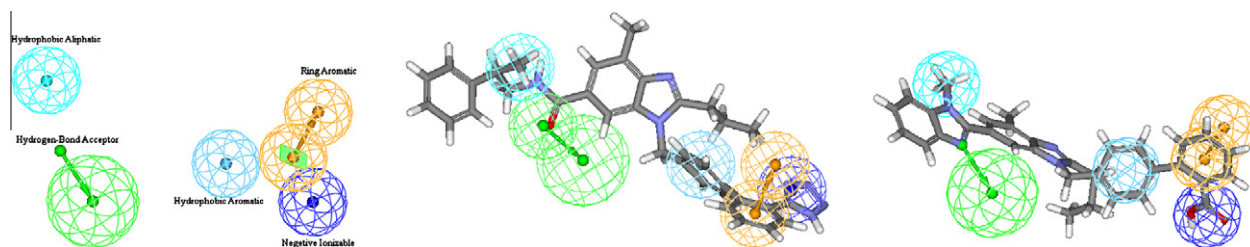


Figure 4. (a) The selected pharmacophore hypothesis; (b) mapping of **6g** with the selected hypothesis; (c) mapping of telmisartan with the selected hypothesis.

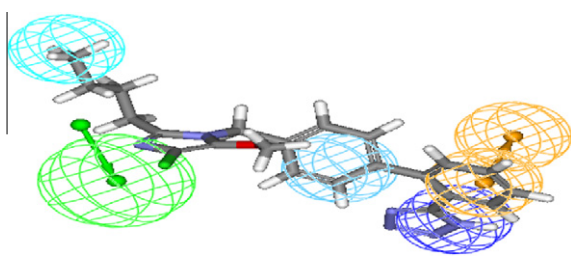


Figure 5. Mapping of losartan with the selected hypothesis.

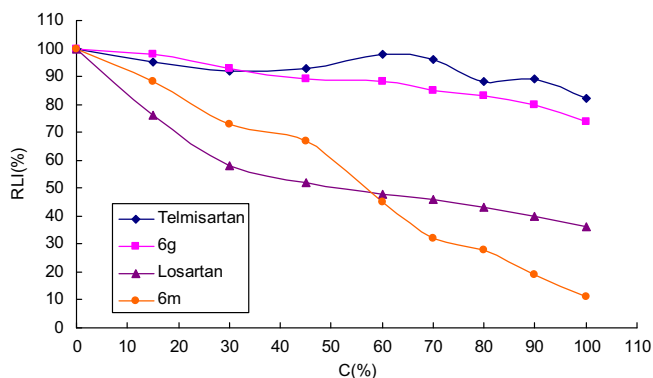


Figure 6. The inhibition tendency of some compounds.

characterised by IR, ¹H NMR, ¹³C NMR and HRMS. Infrared (IR) spectra were recorded on an FTIR spectrometer (Nicolet Magna IR 560) with KBr pellets. ¹H NMR and ¹³C NMR spectra were measured on a Bruker Avance III 400 NMR spectrometer using TMS as an internal standard (chemical shift in ppm). High-resolution mass spectra were recorded on a Bruker Apex IV FTMS spectrometer. Column chromatography was performed with silica gel (200–300 mesh). Thin layer chromatography was performed on high-silica-gel GF₂₅₄ pre-coated plates.

4.1.1. 4-Methyl-2-*n*-propyl-1*H*-benzimidazole-6-carboxylic chloride (**3**)

A suspension of **2** (2.18 g, 10 mmol) in thionyl chloride (20 mL, 276 mmol) was refluxed for 2 h, and then the excess thionyl chloride was removed under a vacuum to provide the crude acid chloride (**3**) as an off-white solid. The crude product **3** was used in the next step without further purification.

4.1.2. General synthetic procedure for 4a–4k

To a stirred suspension of the resulting acid chloride in 60 mL of chloroform at 0 °C was added dropwise to triethylamine (1.52 g, 15 mmol), followed by a solution of one of the substituted amines (10 mmol) in 10 mL of chloroform. The resulting mixture was stirred at 25 °C for 8 h. The reaction mixture was filtered, and the filtrate was washed with brine, saturated sodium bicarbonate solution, brine and water, dried over anhydrous sodium sulphate, filtered, and concentrated under a vacuum. The residue was purified by recrystallisation in ethanol to provide pure product as white solids.

4.1.2.1. N-Benzyl-4-methyl-2-n-propyl-1H-benzimidazole-6-carboxamide (4a). White solid (2.22 g, 72.3% overall from **2**), mp 134–136 °C. IR(KBr), $\nu_{\text{max}}/\text{cm}^{-1}$: 3254, 3183, 2955, 2929, 2870, 1633, 1604, 1548, 1423, 1328, 1233, 1078, 893, 691; ^1H NMR (400 MHz, DMSO) δ : 0.96 (t, $J = 7.2$ Hz, 3H), 1.76 (m, 2H), 2.57 (s, 3H), 2.84 (t, $J = 7.1$ Hz, 2H), 4.32 (s, 2H), 7.06–7.21 (m, 5H), 7.61 (s, 1H), 7.82 (s, 1H), 8.45 (s, 1H); ESIMS(m/z): 308.2 (M+H) $^+$.

4.1.2.2. N-(2-Methoxy)benzyl-4-methyl-2-n-propyl-1H-benzimidazole-6-carboxamide (4b). White solid (2.63 g, 77.9% overall from **2**), mp 129–131 °C. IR(KBr), $\nu_{\text{max}}/\text{cm}^{-1}$: 3187, 3124, 2961, 2931, 2871, 1701, 1598, 1533, 1432, 1320, 1209, 1040, 874, 764, 690; ^1H NMR (400 MHz, DMSO) δ : 0.94 (t, $J = 7.3$ Hz, 3H), 1.76 (m, 2H), 2.56 (s, 3H), 2.83 (t, $J = 7.1$ Hz, 2H), 3.47 (s, 3H), 4.45 (s, 2H), 7.09–7.31 (m, 4H), 7.57 (s, 1H), 7.88 (s, 1H), 8.48 (s, 1H); ESIMS(m/z): 338.2 (M+H) $^+$.

4.1.2.3. N-(3-Methoxy)benzyl-4-methyl-2-n-propyl-1H-benzimidazole-6-carboxamide (4c). White solid (2.52 g, 74.8% overall from **2**), mp 132–134 °C. IR(KBr), $\nu_{\text{max}}/\text{cm}^{-1}$: 3198, 2957, 2927, 2871, 1632, 1604, 1533, 1425, 1311, 1232, 1040, 898, 692; ^1H NMR (400 MHz, DMSO) δ : 0.95 (t, $J = 7.2$ Hz, 3H), 1.77 (m, 2H), 2.55 (s, 3H), 2.86 (t, $J = 7.1$ Hz, 2H), 3.72 (s, 3H), 4.42 (s, 2H), 6.78–7.24 (m, 4H), 7.58 (s, 1H), 7.87 (s, 1H), 8.47 (s, 1H); ESIMS(m/z): 338.2 (M+H) $^+$.

4.1.2.4. N-(4-Methoxy)benzyl-4-methyl-2-n-propyl-1H-benzimidazole-6-carboxamide (4d). White solid (2.41 g, 71.4% overall from **2**), mp 133–135 °C. IR(KBr), $\nu_{\text{max}}/\text{cm}^{-1}$: 3231, 2959, 2931, 2872, 1628, 1603, 1536, 1510, 1430, 1330, 1245, 1179, 1097, 1036, 890, 817, 766; ^1H NMR (400 MHz, DMSO) δ : 0.94 (t, $J = 7.2$ Hz, 3H), 1.79 (m, 2H), 2.56 (s, 3H), 2.87 (t, $J = 7.2$ Hz, 2H), 3.78 (s, 3H), 4.47 (s, 2H), 6.82–7.29 (m, 4H), 7.55 (s, 1H), 7.82 (s, 1H), 8.46 (s, 1H); ESIMS(m/z): 338.2 (M+H) $^+$.

4.1.2.5. N-(3,4-Dimethoxy)benzyl-4-methyl-2-n-propyl-1H-benzimidazole-6-carboxamide (4e). White solid (2.75 g, 75.0% overall from **2**), mp 128–130 °C. IR(KBr), $\nu_{\text{max}}/\text{cm}^{-1}$: 3307, 3197, 2958, 2932, 2872, 1629, 1605, 1539, 1516, 1439, 1314, 1264, 1235, 1138, 1026, 894, 806, 764; ^1H NMR (400 MHz, DMSO) δ : 0.81 (t, $J = 7.3$ Hz, 3H), 1.72 (m, 2H), 2.50 (s, 3H), 2.81 (t, $J = 7.2$ Hz, 2H), 3.71 (s, 3H), 3.79 (s, 3H), 4.43 (s, 2H), 6.99–7.01 (m, 3H), 7.68 (s, 1H), 7.81 (s, 1H); ESIMS(m/z): 368.2 (M+H) $^+$.

4.1.2.6. N-(β -Phenethyl)-4-methyl-2-n-propyl-1H-benzimidazole-6-carboxamide (4f). White solid (2.41 g, 75.1% overall from **2**), mp 152–154 °C. IR(KBr), $\nu_{\text{max}}/\text{cm}^{-1}$: 3341, 3193, 3060, 3025, 2958, 2930, 2872, 1631, 1606, 1545, 1417, 1321, 1233, 1087, 894, 741, 697; ^1H NMR (400 MHz, DMSO) δ : 0.94 (t, $J = 7.2$ Hz, 3H), 1.78 (m, 2H), 2.55 (s, 3H), 2.79 (t, $J = 7.2$ Hz, 2H), 2.85 (t, $J = 7.1$ Hz, 2H), 3.49 (m, 2H), 7.20–7.31 (m, 5H), 7.47 (s, 1H), 7.87 (s, 1H), 8.42 (s, 1H); ESIMS(m/z): 322.2 (M+H) $^+$.

4.1.2.7. N-(2-Methyl-2-phenyl)ethyl-4-methyl-2-n-propyl-1H-benzimidazole-6-carboxamide (4g). White solid (2.67 g, 79.7% overall from **2**), mp 140–142 °C. IR(KBr), $\nu_{\text{max}}/\text{cm}^{-1}$: 3337, 2960, 2931, 2873, 1633, 1606, 1547, 1509, 1417, 1315, 1230, 1098, 1016, 761, 700; ^1H NMR (400 MHz, DMSO) δ : 0.94 (t, $J = 7.2$ Hz, 3H), 1.58 (d, $J = 7.2$ Hz, 3H), 1.78 (m, 2H), 2.56 (s, 3H), 2.84 (t, $J = 7.2$ Hz, 2H), 4.97 (s, 1H), 7.15–7.31 (m, 5H), 7.46 (s, 1H), 7.89 (s, 1H), 8.44 (s, 1H); ESIMS(m/z): 336.2 (M+H) $^+$.

4.1.2.8. N-[β -(3-Methoxy)phenethyl]-4-methyl-2-n-propyl-1H-benzimidazole-6-carboxamide (4h). White solid (2.66 g, 75.7% overall from **2**), mp 148–150 °C. IR(KBr), $\nu_{\text{max}}/\text{cm}^{-1}$: 3342,

3114, 3024, 2962, 2930, 2873, 1608, 1550, 1453, 1315, 1017, 761, 700; ^1H NMR (400 MHz, DMSO) δ : 0.81 (t, $J = 7.2$ Hz, 3H), 1.71 (m, 2H), 2.49 (s, 3H), 2.79 (t, $J = 7.2$ Hz, 2H), 2.89 (t, $J = 7.2$ Hz, 2H), 3.65 (m, 2H), 3.77 (s, 3H), 6.77–7.20 (m, 4H), 7.67 (s, 1H), 7.78 (s, 1H); ESIMS(m/z): 352.2 (M+H) $^+$.

4.1.2.9. N-[β -(4-Methoxy)phenethyl]-4-methyl-2-n-propyl-1H-benzimidazole-6-carboxamide (4i). White solid (2.69 g, 76.6% overall from **2**), mp 149–151 °C. IR(KBr), $\nu_{\text{max}}/\text{cm}^{-1}$: 3337, 2960, 2931, 2873, 1633, 1606, 1547, 1509, 1417, 1315, 1230, 1098, 1016, 761, 700; ^1H NMR (400 MHz, DMSO) δ : 0.98 (t, $J = 7.3$ Hz, 3H), 1.81 (m, 2H), 2.57 (s, 3H), 2.77 (t, $J = 7.2$ Hz, 2H), 2.88 (t, $J = 7.1$ Hz, 2H), 3.40 (m, 2H), 3.67 (s, 3H), 6.84–7.32 (m, 4H), 7.45 (s, 1H), 7.84 (s, 1H); ESIMS(m/z): 352.2 (M+H) $^+$.

4.1.2.10. N-[β -(2,5-Dimethoxy)phenethyl]-4-methyl-2-n-propyl-1H-benzimidazole-6-carboxamide (4j). White solid (2.75 g, 72.4% overall from **2**), mp 145–147 °C. IR(KBr), $\nu_{\text{max}}/\text{cm}^{-1}$: 3330, 3026, 2961, 2932, 2833, 1627, 1595, 1555, 1505, 1419, 1319, 1227, 1045, 890, 807, 703; ^1H NMR (400 MHz, DMSO) δ : 0.95 (t, $J = 7.2$ Hz, 3H), 1.76 (m, 2H), 2.55 (s, 3H), 2.78 (t, $J = 7.2$ Hz, 2H), 2.86 (t, $J = 7.2$ Hz, 2H), 3.48 (m, 2H), 3.70 (s, 3H), 3.76 (s, 3H), 6.94–7.12 (m, 3H), 7.70 (s, 1H), 7.86 (s, 1H); ESIMS(m/z): 382.2 (M+H) $^+$.

4.1.2.11. N-[β -(3,4-Dimethoxy)phenethyl]-4-methyl-2-n-propyl-1H-benzimidazole-6-carboxamide (4k). White solid (3.00 g, 78.7% overall from **2**), mp 147–149 °C. IR(KBr), $\nu_{\text{max}}/\text{cm}^{-1}$: 3247, 3080, 2933, 2871, 1636, 1607, 1595, 1549, 1515, 1441, 1323, 1231, 1141, 1027, 765; ^1H NMR (400 MHz, DMSO) δ : 0.96 (t, $J = 7.2$ Hz, 3H), 1.78 (m, 2H), 2.56 (s, 3H), 2.77 (t, $J = 7.2$ Hz, 2H), 2.87 (t, $J = 7.2$ Hz, 2H), 3.47 (m, 2H), 3.72 (s, 3H), 3.78 (s, 3H), 6.98–7.15 (m, 3H), 7.72 (s, 1H), 7.89 (s, 1H); ESIMS(m/z): 382.2 (M+H) $^+$.

4.1.2.12. N-[β -(2-Fluoro)phenethyl]-4-methyl-2-n-propyl-1H-benzimidazole-6-carboxamide (4l). White solid (2.59 g, 76.3% overall from **2**), mp 133–135 °C. IR(KBr), $\nu_{\text{max}}/\text{cm}^{-1}$: 3341, 3026, 2959, 2931, 2873, 1701, 1607, 1544, 1429, 1322, 1229, 1200, 1097, 896, 756, 697; ^1H NMR (400 MHz, DMSO) δ : 0.95 (t, $J = 7.2$ Hz, 3H), 1.67 (m, 2H), 2.55 (s, 3H), 2.75 (t, $J = 7.2$ Hz, 2H), 2.86 (t, $J = 7.2$ Hz, 2H), 3.53 (m, 2H), 6.93–7.25 (m, 4H), 7.47 (s, 1H), 7.82 (s, 1H); ESIMS(m/z): 340.2 (M+H) $^+$.

4.1.2.13. N-[β -(4-Fluoro)phenethyl]-4-methyl-2-n-propyl-1H-benzimidazole-6-carboxamide (4m). White solid (2.52 g, 74.4% overall from **2**), mp 137–139 °C. IR(KBr), $\nu_{\text{max}}/\text{cm}^{-1}$: 3341, 3026, 2959, 2931, 2873, 1701, 1607, 1544, 1429, 1322, 1229, 1200, 1097, 896, 756, 697; ^1H NMR (400 MHz, DMSO) δ : 0.96 (t, $J = 7.2$ Hz, 3H), 1.69 (m, 2H), 2.56 (s, 3H), 2.78 (t, $J = 7.3$ Hz, 2H), 2.87 (t, $J = 7.2$ Hz, 2H), 3.56 (m, 2H), 6.97–7.23 (m, 4H), 7.46 (s, 1H), 7.84 (s, 1H); ESIMS(m/z): 340.2 (M+H) $^+$.

4.1.3. General synthetic procedure for 5a–5k

To a stirred solution of compound **4** (2 mmol) in 15 mL of dimethylformamide at 0 °C, potassium *tert*-butoxide (2.2 mmol) was added. The mixture was stirred for 30 min at 0 °C, and then 4'-bromomethyl-2-(1-triphenylmethyltetrazole-5-yl)-1,1'-biphenyl (2.1 mmol) was added. After stirring at 25 °C for 12 h, the mixture was poured into water (80 mL) and extracted with ethyl acetate (40 mL \times 3). The combined ethyl acetate layers were washed with brine (50 mL \times 3), dried over anhydrous magnesium sulphate, and concentrated under a reduced pressure to provide an off-white solid. The solid was purified by column chromatography (elution: 1:1 petroleum ether/ethyl acetate) to provide the pure product in the form of a white crystalline powder.

4.1.3.1. *N*-Benzyl-1-[2'-(1-triphenylmethyltetrazole-5-yl)-1,1'-biphenyl-4-yl]methyl-4-methyl-2-*n*-propyl-1*H*-benzimidazole-6-carboxamide (5a). White crystalline powder (1405 mg, 89.7%), mp 156–157 °C. IR(KBr), $\nu_{\max}/\text{cm}^{-1}$: 3299, 1650, 1596, 1541, 1469, 1378, 1284, 1217, 1029; ^1H NMR (400 MHz, CDCl_3) δ : 0.95(t, J = 7.4 Hz, 3H), 1.73–1.83(m, 2H), 2.70(s, 3H), 2.74(t, J = 8.0 Hz, 2H), 4.578 (d, J = 5.60 Hz, 2H), 5.22(s, 2H), 6.35(t, J = 5.4 Hz, 1H), 6.70–7.60(m, 29H), 7.90–7.93(m, 1H); ESIMS(m/z): 784.4($M+H$) $^+$.

4.1.3.2. *N*-(2-Methoxy)benzyl-1-[2'-(1-triphenylmethyltetrazole-5-yl)-1,1'-biphenyl-4-yl]methyl-4-methyl-2-*n*-propyl-1*H*-benzimidazole-6-carboxamide (5b). White crystalline powder (1404 mg, 86.3%), mp 107–109 °C. IR(KBr), $\nu_{\max}/\text{cm}^{-1}$: 3427, 1646, 1599, 1513, 1492, 1448, 1355, 1247, 1120, 1028; ^1H NMR (400 MHz, CDCl_3) δ : 0.94(t, J = 7.4 Hz, 3H), 1.72–1.80(m, 2H), 2.70(s, 3H), 2.74(t, J = 7.8 Hz, 2H), 3.84(s, 3H), 4.60(d, J = 5.6 Hz, 2H), 5.22(s, 2H), 6.58(t, J = 5.6 Hz, 1H), 6.75–7.61(m, 28H), 7.91–7.93(m, 1H); ESIMS(m/z): 814.4($M+H$) $^+$.

4.1.3.3. *N*-(3-Methoxy)benzyl-1-[2'-(1-triphenylmethyltetrazole-5-yl)-1,1'-biphenyl-4-yl]methyl-4-methyl-2-*n*-propyl-1*H*-benzimidazole-6-carboxamide (5c). White crystalline powder (1467 mg, 90.2%), mp 94–96 °C. IR(KBr), $\nu_{\max}/\text{cm}^{-1}$: 3395, 1655, 1598, 1531, 1490, 1357, 1268, 1214, 1186, 1036; ^1H NMR (400 MHz, CDCl_3) δ : 0.95(t, J = 7.4 Hz, 3H), 1.73–1.81(m, 2H), 2.70(s, 3H), 2.74(t, J = 8. Hz, 2H), 3.77(s, 3H), 4.55(d, J = 5.6 Hz, 2H), 5.22(s, 2H), 6.36(t, J = 5.6 Hz, 1H), 6.76–7.59(m, 28H), 7.90–7.92(m, 1H); ESIMS(m/z): 814.4($M+H$) $^+$.

4.1.3.4. *N*-(4-Methoxy)benzyl-1-[2'-(1-triphenylmethyltetrazole-5-yl)-1,1'-biphenyl-4-yl]methyl-4-methyl-2-*n*-propyl-1*H*-benzimidazole-6-carboxamide (5d). White crystalline powder (1427 mg, 87.7%), mp 104–107 °C. IR(KBr), $\nu_{\max}/\text{cm}^{-1}$: 3299, 1650, 1600, 1511, 1468, 1380, 1287, 1187, 1036; ^1H NMR (400 MHz, CDCl_3) δ : 0.94(t, J = 7.4 Hz, 3H), 1.73–1.80(m, 2H), 2.67(s, 3H), 2.74(t, J = 8.0 Hz, 2H), 3.78(s, 3H), 4.51(d, J = 5.6 Hz, 2H), 5.21(s, 2H), 6.32(t, J = 5.6 Hz, 1H), 6.75–7.60(m, 28H), 7.90–7.93(m, 1H); ESIMS(m/z): 814.4($M+H$) $^+$.

4.1.3.5. *N*-(3,4-Dimethoxy)benzyl-1-[2'-(1-triphenylmethyltetrazole-5-yl)-1,1'-biphenyl-4-yl]methyl-4-methyl-2-*n*-propyl-1*H*-benzimidazole-6-carboxamide (5e). White crystalline powder (1167 mg, 69.2%), mp 109–112 °C. IR(KBr), $\nu_{\max}/\text{cm}^{-1}$: 3297, 1641, 1594, 1510, 1447, 1357, 1261, 1188, 1028, 1006, 875, 750, 698; ^1H NMR (400 MHz, CDCl_3) δ : 0.95(t, J = 7.4 Hz, 3H), 1.75–1.81(m, 2H), 2.70(s, 3H), 2.75(t, J = 7.8 Hz, 2H), 3.83(s, 3H), 3.85(s, 3H), 4.51(d, J = 5.6 Hz, 2H), 5.23(s, 2H), 6.32(t, J = 5.6 Hz, 1H), 6.76–7.59(m, 27H), 7.90–7.92(m, 1H); ESIMS(m/z): 844.4($M+H$) $^+$.

4.1.3.6. *N*-(β -Phenethyl)-1-[2'-(1-triphenylmethyltetrazole-5-yl)-1,1'-biphenyl-4-yl]methyl-4-methyl-2-*n*-propyl-1*H*-benzimidazole-6-carboxamide (5f). White crystalline powder (1351 mg, 84.7%), mp 161–162 °C. IR(KBr), $\nu_{\max}/\text{cm}^{-1}$: 3329, 1653, 1595, 1541, 1470, 1358, 1290, 1216, 1032; ^1H NMR (400 MHz, CDCl_3) δ : 0.95(t, J = 7.4 Hz, 3H), 1.64–1.83(m, 2H), 2.69(s, 3H), 2.75(t, J = 7.8 Hz, 2H), 2.89(t, J = 7.0 Hz, 2H), 3.67(m, 2H), 5.22(s, 2H), 6.09(t, J = 5.8 Hz, 1H), 6.76–7.51(m, 29H), 7.90–7.92(m, 1H); ESIMS(m/z): 798.4($M+H$) $^+$.

4.1.3.7. *N*-(2-Methyl-2-phenyl)ethyl-1-[2'-(1-triphenylmethyltetrazole-5-yl)-1,1'-biphenyl-4-yl]methyl-4-methyl-2-*n*-propyl-1*H*-benzimidazole-6-carboxamide (5g). White crystalline powder (1229 mg, 75.7%), mp 102–104 °C. IR(KBr), $\nu_{\max}/\text{cm}^{-1}$: 3378, 1653, 1596, 1540, 1469, 1356, 1286, 1215, 1033; ^1H NMR

(400 MHz, CDCl_3) δ : 0.94(t, J = 7.4 Hz, 3H), 1.32(d, J = 6.8 Hz, 1H), 1.74–1.81(m, 2H), 2.66 (s, 3H), 2.72(t, J = 9.2 Hz, 2H), 3.02–3.08(m, 1H), 3.32–3.39 (m, 1H), 5.20(s, 2H), 5.95(s, 1H), 6.75–7.51(m, 29H), 7.90–7.93(m, 1H); ESIMS(m/z): 812.4($M+H$) $^+$.

4.1.3.8. *N*-(β -(3-Methoxy)phenethyl)-1-[2'-(1-triphenylmethyltetrazole-5-yl)-1,1'-biphenyl-4-yl]methyl-4-methyl-2-*n*-propyl-1*H*-benzimidazole-6-carboxamide (5h). White crystalline powder (1210 mg, 73.1%), mp 94–97 °C. IR(KBr), $\nu_{\max}/\text{cm}^{-1}$: 3388, 1652, 1596, 1538, 1488, 1352, 1272, 1215, 1190, 1033; ^1H NMR (400 MHz, CDCl_3) δ : 0.95(t, J = 7.4 Hz, 3H), 1.75–1.81(m, 2H), 2.69(s, 3H), 2.75(t, J = 8.0 Hz, 2H), 2.87(t, J = 7.0 Hz, 2H), 3.61–3.66(m, 2H), 3.76(s, 3H), 5.22(s, 2H), 6.12(d, J = 4.8 Hz, 1H), 6.76–7.52(m, 28H), 7.90–7.92(m, 1H); ESIMS(m/z): 828.4($M+H$) $^+$.

4.1.3.9. *N*-(β -(4-Methoxy)phenethyl)-1-[2'-(1-triphenylmethyltetrazole-5-yl)-1,1'-biphenyl-4-yl]methyl-4-methyl-2-*n*-propyl-1*H*-benzimidazole-6-carboxamide (5i). White crystalline powder (1174 mg, 70.9%), mp 105–107 °C. IR(KBr), $\nu_{\max}/\text{cm}^{-1}$: 3327, 1653, 1595, 1539, 1470, 1357, 1240, 1215, 1033; ^1H NMR (400 MHz, CDCl_3) δ : 0.95(t, J = 7.4 Hz, 3H), 1.75–1.81(m, 2H), 2.69(s, 3H), 2.75(t, J = 7.8 Hz, 2H), 2.83(t, J = 7.0 Hz, 2H), 3.58–3.63(m, 2H), 3.77(s, 3H), 5.22(s, 2H), 6.08(t, J = 5.60 Hz, 1H), 6.77–7.52(m, 28H), 7.90–7.92(m, 1H); ESIMS(m/z): 828.4($M+H$) $^+$.

4.1.3.10. *N*-(β -(2,5-Dimethoxy)phenethyl)-1-[2'-(1-triphenylmethyltetrazole-5-yl)-1,1'-biphenyl-4-yl]methyl-4-methyl-2-*n*-propyl-1*H*-benzimidazole-6-carboxamide (5j). White crystalline powder (1497 mg, 87.3%), mp 176–178 °C. IR(KBr), $\nu_{\max}/\text{cm}^{-1}$: 3293, 1646, 1596, 1540, 1497, 1444, 1348, 1281, 1223, 1032; ^1H NMR (400 MHz, CDCl_3) δ : 0.94(t, J = 7.4 Hz, 3H), 1.70(s, 3H), 1.72–1.82(m, 2H), 2.70–2.75(m, 5H), 2.91(t, J = 6.4 Hz, 2H), 3.59–3.64(m, 2H), 3.72(s, 3H), 3.77(s, 3H), 5.22(s, 2H), 6.58(t, J = 4.8 Hz, 1H), 6.71–7.58(m, 27H), 7.90–7.92(m, 1H); ESIMS(m/z): 858.4($M+H$) $^+$.

4.1.3.11. *N*-(β -(3,4-Dimethoxy)phenethyl)-1-[2'-(1-triphenylmethyltetrazole-5-yl)-1,1'-biphenyl-4-yl]methyl-4-methyl-2-*n*-propyl-1*H*-benzimidazole-6-carboxamide (5k). White crystalline powder (1337 mg, 78.0%), mp 127–128 °C. IR(KBr), $\nu_{\max}/\text{cm}^{-1}$: 3356, 1652, 1594, 1540, 1490, 1357, 1262, 1236, 1155, 1028; ^1H NMR (400 MHz, CDCl_3) δ : 0.94(t, J = 7.4 Hz, 3H), 1.73–1.88(m, 3H), 2.68(s, 3H), 2.74(t, J = 7.8 Hz, 2H), 2.83(t, J = 7.0 Hz, 2H), 3.59–3.64(m, 2H), 3.811(s, 3H), 3.843(s, 3H), 5.22(s, 2H), 6.10–6.25(br, 1H), 6.73–7.55(m, 27H), 7.89–7.91(m, 1H); ESIMS(m/z): 858.4($M+H$) $^+$.

4.1.3.12. *N*-(β -(2-Fluoro)phenethyl)-1-[2'-(1-triphenylmethyltetrazole-5-yl)-1,1'-biphenyl-4-yl]methyl-4-methyl-2-*n*-propyl-1*H*-benzimidazole-6-carboxamide (5l). White crystalline powder (1076 mg, 66.0%), mp 184–186 °C. IR(KBr), $\nu_{\max}/\text{cm}^{-1}$: 3378, 1655, 1597, 1536, 1491, 1452, 1355, 1272, 1227, 1034; ^1H NMR (400 MHz, CDCl_3) δ : 0.95(t, J = 7.4 Hz, 3H), 1.73–1.83(m, 2H), 2.70(s, 3H), 2.75(t, J = 8.0 Hz, 2H), 2.94(t, J = 6.8 Hz, 2H), 3.61–3.66(m, 2H), 5.22(s, 2H), 6.17(s, 1H), 6.77–7.52(m, 28H), 7.90–7.92(m, 1H); ESIMS(m/z): 816.4($M+H$) $^+$.

4.1.3.13. *N*-(β -(4-Fluoro)phenethyl)-1-[2'-(1-triphenylmethyltetrazole-5-yl)-1,1'-biphenyl-4-yl]methyl-4-methyl-2-*n*-propyl-1*H*-benzimidazole-6-carboxamide (5m). White crystalline powder (1290 mg, 79.1%), mp 181–183 °C. IR(KBr), $\nu_{\max}/\text{cm}^{-1}$: 3323, 1654, 1597, 1541, 1509, 1470, 1445, 1357, 1289, 1218; ^1H NMR (400 MHz, CDCl_3) δ : 0.95(t, J = 7.4 Hz, 3H), 1.73–1.81(m, 2H), 2.69(s, 3H), 2.75(t, J = 7.8 Hz, 2H), 2.85(t, J = 7.2 Hz, 2H), 3.56–3.62(m, 2H), 5.23(s, 2H), 6.09(t, J = 5.4 Hz, 1H), 6.77–7.51(m, 28H), 7.89–7.91(m, 1H); ESIMS(m/z): 816.4($M+H$) $^+$.

4.1.4. General Synthetic Procedure for 6a–6k

A solution of one of **5a–5k** (1 mmol), 40 mL of tetrahydrofuran, 40 mL of methanol, and 9 mL of 3 N aqueous hydrochloric acid were stirred at 25 °C for 12 h. The solution was adjusted to pH 12 with 1 N aqueous sodium hydroxide, and the organic solvents were removed under a vacuum. The residual liquid was filtered, and the filtrate was adjusted to pH 6–7 with 3 N aqueous hydrochloric acid. The resulting precipitate was filtered, washed with water, dried, and then recrystallised in ethyl acetate/ethanol (4:1) to afford the target product as a white powder.

4.1.4.1. N-Benzyl-1-[2'-(1H-tetrazol-5-yl)-1,1'-biphenyl-4-yl]methyl-4-methyl-2-n-propyl-1H-benzimidazole-6-carboxamide (6a). White powder (447 mg, 82.6%), mp 185–187 °C, IR(KBr), $\nu_{\max}/\text{cm}^{-1}$: 3286, 1638, 1590, 1542, 1457, 1350, 1276, 1209, 1080, 1004, 875, 758; ^1H NMR (400 MHz, DMSO- d_6) δ : 0.95(t, J = 7.4 Hz, 3H), 1.73–1.78(m, 2H), 2.56(s, 3H), 2.80(t, J = 7.6 Hz, 2H), 4.48 (d, J = 6.0 Hz, 2H), 5.47(s, 2H), 6.90–7.61(m, 14H), 7.93(s, 1H), 8.93(t, J = 5.6 Hz, 1H); HRMS calcd for $\text{C}_{33}\text{H}_{32}\text{N}_7\text{O}[\text{M}+\text{H}]^+$ 542.2663, found 542.2656.

4.1.4.2. N-(2-Methoxy)benzyl-1-[2'-(1H-tetrazol-5-yl)-1,1'-biphenyl-4-yl]methyl-4-methyl-2-n-propyl-1H-benzimidazole-6-carboxamide (6b). White powder (507 mg, 88.7%), mp 192–193 °C, IR(KBr), $\nu_{\max}/\text{cm}^{-1}$: 3263, 1635, 1591, 1536, 1492, 1458, 1392, 1275, 1240, 1119, 1026, 877, 754; ^1H NMR (400 MHz, DMSO- d_6) δ : 0.95(t, J = 7.4 Hz, 3H), 1.71–1.80(m, 2H), 2.57(s, 3H), 2.80(t, J = 7.4 Hz, 2H), 3.81(s, 3H), 4.45 (d, J = 5.6 Hz, 2H), 5.47(s, 2H), 6.87–7.52(m, 12H), 7.62(s, 1H), 7.95(s, 1H), 8.71(t, J = 5.6 Hz, 1H); ^{13}C NMR (100 MHz, DMSO- d_6) δ : 13.99, 14.27, 16.68, 20.69, 20.95, 28.90, 46.02, 55.49, 59.94, 107.36, 110.57, 120.29, 121.49, 125.60, 127.01, 127.32, 127.53, 127.62, 127.97, 128.07, 129.63, 130.29, 130.67, 134.84, 135.08, 140.19, 140.93, 143.98, 156.72, 156.78, 166.93; HRMS calcd for $\text{C}_{34}\text{H}_{34}\text{N}_7\text{O}_2[\text{M}+\text{H}]^+$ 572.2769, found 572.2757.

4.1.4.3. N-(3-Methoxy)benzyl-1-[2'-(1H-tetrazol-5-yl)-1,1'-biphenyl-4-yl]methyl-4-methyl-2-n-propyl-1H-benzimidazole-6-carboxamide (6c). White powder (431 mg, 75.4%), mp 181–183 °C, IR(KBr), $\nu_{\max}/\text{cm}^{-1}$: 3274, 1635, 1595, 1542, 1458, 1360, 1263, 1212, 1149, 1040, 1009, 869, 759; ^1H NMR (400 MHz, DMSO- d_6) δ : 0.95(t, J = 7.4 Hz, 3H), 1.71–1.80(m, 2H), 2.56(s, 3H), 2.80(t, J = 7.6 Hz, 2H), 3.71(s, 3H), 4.45(d, J = 5.6 Hz, 2H), 5.47(s, 2H), 6.78–7.60(m, 13H), 7.93(s, 1H), 8.90(t, J = 5.8 Hz, 1H); ^{13}C NMR (100 MHz, DMSO- d_6) δ : 14.00, 14.27, 16.67, 20.69, 20.95, 28.89, 42.81, 46.03, 55.13, 59.94, 107.34, 112.17, 113.19, 119.64, 121.46, 125.62, 127.07, 127.65, 128.01, 128.10, 129.50, 129.63, 130.31, 130.67, 131.11, 134.83, 135.09, 140.19, 140.90, 141.74, 144.00, 156.81, 159.45, 159.81, 166.80, 170.53; HRMS calcd for $\text{C}_{34}\text{H}_{34}\text{N}_7\text{O}_2[\text{M}+\text{H}]^+$ 572.2769, found 572.2757.

4.1.4.4. N-(4-Methoxy)benzyl-1-[2'-(1H-tetrazol-5-yl)-1,1'-biphenyl-4-yl]methyl-4-methyl-2-n-propyl-1H-benzimidazole-6-carboxamide (6d). White powder (472 mg, 82.6%), mp 197–198 °C, IR(KBr), $\nu_{\max}/\text{cm}^{-1}$: 3285, 1636, 1585, 1536, 1512, 1458, 1347, 1294, 1246, 1174, 1031, 1006, 817, 759; ^1H NMR (400 MHz, DMSO- d_6) δ : 0.93(t, J = 7.4 Hz, 3H), 1.67–1.76(m, 2H), 2.56(s, 3H), 2.79(t, J = 7.6 Hz, 2H), 3.72(s, 3H), 4.41(d, J = 5.6 Hz, 2H), 5.51(s, 2H), 6.87–7.67(m, 13H), 7.91(s, 1H), 8.82(t, J = 5.8 Hz, 1H); ^{13}C NMR (100 MHz, DMSO- d_6) δ : 13.97, 14.27, 16.66, 20.67, 20.95, 28.87, 42.33, 45.91, 55.22, 59.94, 170.50, 113.84, 121.33, 123.64, 126.39, 127.59, 128.00, 128.18, 128.82, 129.41, 130.79, 131.23, 132.04, 134.83, 136.44, 138.65, 141.13, 143.85, 155.10, 156.78, 158.34, 166.65; HRMS calcd for $\text{C}_{34}\text{H}_{34}\text{N}_7\text{O}_2[\text{M}+\text{H}]^+$ 572.2769, found 572.2757.

4.1.4.5. N-(3,4-Dimethoxy)benzyl-1-[2'-(1H-tetrazol-5-yl)-1,1'-biphenyl-4-yl]methyl-4-methyl-2-n-propyl-1H-benzimidazole-6-carboxamide (6e). White powder (433 mg, 72.0%), mp 194–196 °C, IR(KBr), $\nu_{\max}/\text{cm}^{-1}$: 3239, 1368, 1594, 1541, 1515, 1459, 1357, 1265, 1232, 1139, 1025, 853, 803, 761; ^1H NMR (400 MHz, DMSO- d_6) δ : 0.94(t, J = 7.4 Hz, 3H), 1.70–1.77(m, 2H), 2.55(s, 3H), 2.79(t, J = 7.4 Hz, 2H), 3.70(s, 6H), 4.40(d, J = 5.6 Hz, 2H), 5.46(s, 2H), 6.82–7.06(m, 7H), 7.29–7.59(m, 5H), 7.91(s, 1H), 8.82(t, J = 5.2 Hz, 1H); HRMS calcd for $\text{C}_{35}\text{H}_{36}\text{N}_7\text{O}_3[\text{M}+\text{H}]^+$ 602.2874, found 602.2863.

4.1.4.6. N-(β -Phenethyl)-1-[2'-(1H-tetrazol-5-yl)-1,1'-biphenyl-4-yl]methyl-4-methyl-2-n-propyl-1H-benzimidazole-6-carboxamide (6f). White powder (459 mg, 82.6%), mp 176–178 °C, IR(KBr), $\nu_{\max}/\text{cm}^{-1}$: 3296, 1639, 1591, 1542, 1456, 1404, 1351, 1275, 1215, 1086, 1006, 839, 758; ^1H NMR (400 MHz, DMSO- d_6) δ : 0.94(t, J = 7.40 Hz, 3H), 1.67–1.77(m, 2H), 2.56(s, 3H), 2.79 (t, J = 7.60 Hz, 2H), 2.85(t, J = 7.60 Hz, 2H), 3.46–3.51(m, 2H), 5.50(s, 2H), 7.0–7.30(m, 9H), 7.49–7.67(m, 5H), 7.84(s, 1H), 8.41–8.44(t, J = 5.60 Hz, 1H); HRMS calcd for $\text{C}_{34}\text{H}_{34}\text{N}_7\text{O}[\text{M}+\text{H}]^+$ 556.2819, found 556.2808.

4.1.4.7. N-(2-Phenyl)propyl-1-[2'-(1H-tetrazol-5-yl)-1,1'-biphenyl-4-yl]methyl-4-methyl-2-n-propyl-1H-benzimidazole-6-carboxamide (6g). White powder (501 mg, 88.0%), mp 178–180 °C, IR(KBr), $\nu_{\max}/\text{cm}^{-1}$: 3285, 1640, 1593, 1539, 1456, 1404, 1349, 1270, 1212, 1119, 1021, 875, 757; ^1H NMR (400 MHz, DMSO- d_6) δ : 0.93(t, J = 7.4 Hz, 3H), 1.23 (d, J = 6.8 Hz, 3H), 1.67–1.77(m, 2H), 2.55 (s, 3H), 2.79(t, J = 7.6 Hz, 2H), 3.07–3.13(m, 1H), 3.36–3.47 (m, 2H), 5.50(s, 2H), 7.0–7.30 (m, 9H), 7.50–7.68(m, 5H), 7.82(s, 1H), 8.33–8.36(t, J = 5.6 Hz, 1H); HRMS calcd for $\text{C}_{35}\text{H}_{36}\text{N}_7\text{O}[\text{M}+\text{H}]^+$ 570.2976, found 570.2968.

4.1.4.8. N-[β -(3-Methoxy)phenethyl]-1-[2'-(1H-tetrazol-5-yl)-1,1'-biphenyl-4-yl] methyl-4-methyl-2-n-propyl-1H-benzimidazole-6-carboxamide (6h). White powder (469 mg, 80.1%), mp 164–166 °C, IR(KBr), $\nu_{\max}/\text{cm}^{-1}$: 3427, 1637, 1593, 1541, 1457, 1352, 1262, 1215, 1149, 1093, 875, 757; ^1H NMR (400 MHz, DMSO- d_6) δ : 0.95(t, J = 7.4 Hz, 3H), 1.71–1.78(m, 2H), 2.55(s, 3H), 2.78–2.84(m, 4H), 3.45–3.52(m, 2H), 3.70(s, 3H), 5.47(s, 2H), 6.74–7.56(m, 13H), 7.84(s, 1H), 8.44(t, J = 5.6 Hz, 1H); ^{13}C NMR (100 MHz, DMSO- d_6) δ : 13.99, 14.27, 16.67, 20.70, 20.95, 28.89, 35.43, 46.00, 55.03, 59.94, 107.21, 111.76, 114.38, 121.09, 121.34, 125.66, 127.14, 127.55, 128.35, 129.49, 129.62, 130.34, 130.69, 134.77, 135.17, 140.26, 140.75, 141.43, 143.87, 156.72, 159.44, 159.53, 166.77; HRMS calcd for $\text{C}_{35}\text{H}_{36}\text{N}_7\text{O}_2[\text{M}+\text{H}]^+$ 586.2925, found 586.2915.

4.1.4.9. N-[β -(4-Methoxy)phenethyl]-1-[2'-(1H-tetrazol-5-yl)-1,1'-biphenyl-4-yl]methyl-4-methyl-2-n-propyl-1H-benzimidazole-6-carboxamide (6i). White powder (447 mg, 76.4%), mp 180–182 °C, IR(KBr), $\nu_{\max}/\text{cm}^{-1}$: 3274, 1637, 1593, 1544, 1511, 1459, 1352, 1297, 1245, 1176, 1034, 877, 820, 757; ^1H NMR (400 MHz, DMSO- d_6) δ : 0.91(t, J = 7.4 Hz, 3H), 1.68–1.74(m, 2H), 2.54(s, 3H), 2.75–2.80(m, 4H), 3.40–3.45 (m, 2H), 3.68(s, 3H), 5.49(s, 2H), 6.81–7.15(m, 8H), 7.48–7.66(m, 5H), 7.83 (s, 1H), 8.38(t, J = 5.2 Hz, 1H); ^{13}C NMR (100 MHz, DMSO- d_6) δ : 13.97, 16.67, 20.69, 28.87, 34.56, 45.92, 55.13, 59.94, 107.37, 113.94, 121.22, 123.68, 126.39, 127.54, 128.00, 128.42, 129.41, 129.77, 130.77, 131.21, 131.67, 134.78, 136.42, 138.68, 141.12, 143.78, 156.71, 157.83, 166.72; HRMS calcd for $\text{C}_{35}\text{H}_{36}\text{N}_7\text{O}_2[\text{M}+\text{H}]^+$ 586.2925, found 586.2913.

4.1.4.10. N-[β -(2,5-Dimethoxy)phenethyl]-1-[2'-(1H-tetrazol-5-yl)-1,1'-biphenyl-4-yl]methyl-4-methyl-2-n-propyl-1H-benzimidazole-6-carboxamide (6j). White powder (489 mg,

79.5%), mp 129–131 °C, IR(KBr), $\nu_{\max}/\text{cm}^{-1}$: 3373, 1626, 1588, 1541, 1501, 1459, 1347, 1273, 1224, 1152, 1039, 877, 762; ^1H NMR (400 MHz, DMSO- d_6) δ : 0.93(t, J = 7.4 Hz, 3H), 1.69–1.75(m, 2H), 2.54(s, 3H), 2.76–2.81(m, 4H), 3.41–3.46(m, 2H), 3.63(s, 3H), 3.70(s, 3H), 5.47(s, 2H), 6.70–7.06(m, 7H), 7.40–7.60(m, 5H), 7.84(s, 1H), 8.36(t, J = 5.6 Hz, 1H); ^{13}C NMR (100 MHz, DMSO- d_6) δ : 13.98, 14.27, 16.67, 20.68, 20.95, 28.88, 30.11, 45.92, 55.39, 55.97, 59.94, 107.26, 111.74, 111.80, 116.40, 121.29, 126.08, 126.56, 127.51, 127.63, 128.42, 128.75, 129.49, 130.01, 130.60, 130.73, 134.79, 135.92, 139.54, 140.77, 143.82, 151.57, 153.16, 156.69, 157.00, 166.72; HRMS calcd for $\text{C}_{36}\text{H}_{38}\text{N}_7\text{O}_3[\text{M}+\text{H}]^+$ 616.3031, found 616.3021.

4.1.4.11. *N*-[β -(3,4-Dimethoxy)phenethyl]-1-[2'-(1*H*-tetrazol-5-yl)-1,1'-biphenyl-4-yl]methyl-4-methyl-2-*n*-propyl-1*H*-benzimidazole-6-carboxamide (6k). White powder (453 mg, 73.6%), mp 185–186 °C, IR(KBr), $\nu_{\max}/\text{cm}^{-1}$: 3235, 1640, 1593, 1548, 1514, 1458, 1351, 1261, 1139, 1025, 877, 760; ^1H NMR (400 MHz, DMSO- d_6) δ : 0.95(t, J = 7.4 Hz, 3H), 1.69–1.79(m, 2H), 2.55(s, 3H), 2.76–2.81(m, 4H), 3.40–3.51(m, 2H), 3.69(d, J = 2.0 Hz, 6H), 5.48(s, 2H), 6.72–7.08(m, 7H), 7.37–7.59(m, 5H), 7.84(s, 1H), 8.40(t, J = 5.6 Hz, 1H); ^{13}C NMR (100 MHz, DMSO- d_6) δ : 13.98, 14.27, 16.67, 20.69, 20.95, 28.88, 34.95, 41.34, 45.97, 55.48, 107.25, 112.08, 112.72, 120.63, 121.29, 125.90, 127.44, 127.54, 128.23, 128.40, 129.3155.48, 55.68, 59.95, 129.54, 130.49, 130.71, 132.31, 134.78, 135.60, 140.04, 140.55, 143.84, 147.36, 148.76, 156.72, 156.72, 158.04, 166.75; HRMS calcd for $\text{C}_{36}\text{H}_{38}\text{N}_7\text{O}_3[\text{M}+\text{H}]^+$ 616.3031, found 616.3021.

4.1.4.12. *N*-[β -(2-Fluoro)phenethyl]-1-[2'-(1*H*-tetrazol-5-yl)-1,1'-biphenyl-4-yl]methyl-4-methyl-2-*n*-propyl-1*H*-benzimidazole-6-carboxamide (6l). White powder (458 mg, 79.9%), mp 183–184 °C, IR(KBr), $\nu_{\max}/\text{cm}^{-1}$: 3286, 1632, 1593, 1544, 1486, 1454, 1349, 1278, 1229, 1108, 1009, 757; ^1H NMR (400 MHz, DMSO- d_6) δ : 0.94(t, J = 7.4 Hz, 3H), 1.67–1.77(m, 2H), 2.55(s, 3H), 2.79(t, J = 7.6 Hz, 2H), 2.89(t, J = 7.4 Hz, 2H), 3.47–3.52(m, 2H), 5.50(s, 2H), 7.08–7.33(m, 8H), 7.50–7.67(m, 5H), 7.84(s, 1H), 8.46(t, J = 5.6 Hz, 1H); ^{13}C NMR (100 MHz, DMSO- d_6) δ : 13.97, 14.27, 16.67, 20.69, 20.95, 28.87, 45.91, 59.94, 107.38, 115.18, 115.40, 121.22, 123.71, 124.51, 124.54, 126.26, 126.40, 127.55, 128.00, 128.33, 128.40, 128.48, 129.41, 130.78, 131.21, 131.30, 131.44, 134.77, 137.41, 138.69, 141.12, 143.82, 156.73, 159.72, 162.14, 166.80; HRMS calcd for $\text{C}_{34}\text{H}_{33}\text{FN}_7\text{O}[\text{M}+\text{H}]^+$ 574.2725, found 574.2714.

4.1.4.13. *N*-[β -(4-Fluoro)phenethyl]-1-[2'-(1*H*-tetrazol-5-yl)-1,1'-biphenyl-4-yl]methyl-4-methyl-2-*n*-propyl-1*H*-benzimidazole-6-carboxamide (6m). White powder (388 mg, 67.7%), mp 188–190 °C, IR(KBr), $\nu_{\max}/\text{cm}^{-1}$: 3230, 1637, 1593, 1544, 1508, 1456, 1404, 1349, 1275, 1219, 1155, 1006, 817, 759; ^1H NMR (400 MHz, DMSO- d_6) δ : 0.96(t, J = 7.2 Hz, 3H), 1.71–1.79(m, 2H), 2.55(s, 3H), 2.79–2.85(m, 4H), 3.44–3.49(m, 2H), 5.47(s, 2H), 6.90–7.56(m, 13H), 7.83(s, 1H), 8.45(t, J = 5.6 Hz, 1H); ^{13}C NMR (100 MHz, DMSO- d_6) δ : 13.99, 14.27, 16.68, 20.71, 20.95, 28.88, 34.52, 41.15, 46.02, 59.94, 107.21, 115.04, 115.25, 121.34, 125.58, 127.06, 127.56, 128.06, 128.29, 129.64, 130.30, 130.56, 130.64, 130.67, 131.23, 134.67, 135.06, 135.97, 136.00, 140.17, 140.94, 143.89, 156.73, 159.77, 159.90, 162.18, 166.79, 170.53; HRMS calcd for $\text{C}_{34}\text{H}_{33}\text{FN}_7\text{O}[\text{M}+\text{H}]^+$ 574.2725, found 574.2714.

4.2. Procedure for the receptor binding assay

The AT₁ receptor binding assay was carried out by competitive displacement of the binding of [^{125}I] Sar¹ Ile⁸-Ang II with the angiotensin AT₁ receptor as described previously.¹⁸ Each 180- μL incubation contained the following: [^{125}I] Sar¹ Ile⁸-Ang II (25 pM), AT₁

receptor (25 μg) and standard or test compounds. The binding was performed at 37 °C for 180 min in 96-well filtration plates (Costar, USA) and was terminated by rapid vacuum filtration using a vacuum device; dried filter disks were punched out and counted in a gamma counter. The IC₅₀ values were estimated from the linear portion of the competition curves.

4.3. Procedure for angiotensin II receptor functional antagonism in rabbit aorta strips

Japanese White Rabbits (2–3 kg body weight, Vitalriver Company, China) were killed by cervical dislocation after a slight anaesthesia with a 20% Urethane solution. The thoracic aorta was carefully dissected out and placed in ice-cold Krebs-Henseleit solution of the following composition (mM): NaCl 118; KCl 4.7; KH₂PO₄ 1.2; MgSO₄·7H₂O 1.17; CaCl₂·2H₂O 2.5; NaHCO₃ 25; glucose 11.1.²⁹ It was cut into helical strips that were 3–4 mm wide and 15–20 mm long. These strips were mounted in 10-mL tissue baths, the tissue baths were kept at 37 °C and aerated with 95% O₂ and 5% CO₂. Each strip was connected to a force transducer, and the changes in the isometric tension were recorded by a four-channel recorder (Medlab-U/4c501, China). The tissues were allowed to equilibrate for 1 h and were washed every 15 min. At the beginning of the experiment, a 67 mM KCl solution was administered to check the sensitivity of the preparations as well as to determine their maximal contractile response. After a 30 min washout, test substances or their respective vehicles were added. Sixty minutes later, cumulative concentration–response curves of angiotensin II were obtained. Only one curve was obtained from each strip, and the contractile response was expressed as a percentage (%) of the maximal contraction achieved with KCl. The pA₂ values were calculated using Schild's plot.³⁰ The antagonist potency was evaluated by the estimation of the pA₂ values.

4.4. Procedure for oral activity in the spontaneously hypertensive rats (SHR)

Male SHR aged 19–21 weeks were used in this study. Six animals served as controls and received the vehicle (10 mL/Kg). The hypertensive animals were divided into two groups (n = 6). Group 1 received losartan (standard drug: 10 mg/kg), and group 2 was given the same doses of the tested compound **6i**. Both the vehicle and test compound were given by oral administration.³¹ Blood pressure and heart rate were measured by tail plethysmography (BP-98A, Softron, Japan) after a warming period in unanesthetised rats. The BP measurements required only a few minutes per individual rat. All data were expressed as means \pm SEM.³²

4.5. Procedure for preliminary toxicity evaluation

The preliminary toxicity evaluation was performed on a water toxicity analyser (BHP 9511, Beijing Hamamatsu Inc.) based on the inhibition of *P. phosphoreum* (T3 mutation), which was supplied by the Institute of Soil Science, Academia Sinica, Nanjing, PR China in the form of a freeze-dried powder. For each test, a serial dilution of the compounds was prepared in 2% saline water according to the pre-test. In addition, a series of saline solutions containing 10⁶ colony units of *P. phosphoreum* was prepared in glass cuvettes by pipetting 10 mL of the reconstituted bacterial suspension into 500 mL of a 2% saline solution. These solutions were incubated for 15 min. and measured. The toxicity of the treated compounds was recorded after 15 min. of exposure to the tested sample. The results of the Microtox test are expressed in terms of LC₅₀ values representing the concentration in water that inhibits 50% of a test batch of *P. phosphoreum*.

4.6. Molecular modelling

Molecular modelling studies were performed using a Silicon Graphics desktop (SGI) Fuel work station. The training set was selected as described above, and the pharmacophore model for the AT₁ receptor antagonists was generated using the HipHop module in Discovery Studio, version 2.0, from Accelrys Inc. The molecules were built in a 3D window, and the conformational models for each molecule were generated using the diverse conformation module. Then the resulting sd files were used to generate the common feature hypotheses using the HipHop module by default. Through these experiments, we specified the features that are crucial for binding with the Ang II receptor, and our results are in agreement with the literature.^{22,23}

Acknowledgements

Financial support of this work was provided by the National Technological Project of the Manufacture and Innovation of Key New Drugs(2009ZX09103-143). We also thank Beijing Hamamatsu Photon Technique Inc. for the providing of the toxicity test instrument.

References and notes

1. Akira, M.; Yuki, N.; Atsushi, A.; Motohiro, T.; Takuma, S. *J. Med. Chem.* **1993**, *34*, 2919.
2. Timmermans, P. B. *Hypertens. Res.* **1999**, *22*, 147.
3. Porrello, E. R.; Delbridge, L. M. D.; Thomas, W. G. *Front Biosci.* **2009**, *14*, 958.
4. Claude, A. B.; Pierre, M. P.; Bernard, P. F.; Yvette, A. M.; Jean-Louis, A. A.; Jacques, C.; Frederique, H.; Claude, F. M.; Joelle, E. T.; Marie-Aimee, V.; Jean, G.; Pierre, R. G.; Colette, A. L.; Alain, R.; Catherine, F.; Cazaubon; Jean-Claude Brelhère; Gerard Le Fur; Dino, N. *J. Med. Chem.* **1993**, *36*, 3371.
5. George, A.; Panagiota, R.; Amalia, R.; Serdar, D.; Maria-Eleni, A.; Konstantinos, K.; Demetrios, V.; Thomas, M.; John, M. *J. Comput. Aided Mol. Des.* **2010**, *24*, 749.
6. Keiji, K.; Yasuhisa, K.; Eiko, I.; Yoshihiro, S.; Yoshiyuki, I.; Yoshiyasu, F.; Kohei, N.; Takehiko, N. *J. Med. Chem.* **1993**, *36*, 2182.
7. Guo, X. Z.; Shi, L.; Wang, R.; Liu, X. X.; Li, B. G.; Lu, X. X. *Bioorg. Med. Chem.* **2008**, *16*, 10301.
8. Sachinidis, A.; El-Haschimi, K.; Ko, Y.; Seul, C.; Epping, P.; Vetter, H. *Eur. J. Pharmacol.* **1996**, *307*, 121.
9. Uwe, J. R.; Gerhard, M.; Berthold, N.; Kai, M. H.; Helmut, W.; Michael, E.; Jacobus, C. A.; Wolfgang, W.; Norbert, H. H. *J. Med. Chem.* **1993**, *36*, 4040.
10. Kubo, K.; Kohara, Y.; Yoshimura, Y.; Inada, Y.; Shibouta, Y.; Furukawa, Y.; Kato, T.; Nishikawa, K.; Naka, T. *J. Med. Chem.* **1993**, *36*, 2343.
11. Bali, A.; Bansal, Y.; Sugumaran, M.; Jatinder, S. S.; Balakumar, P.; Kaur, G.; Bansal, G.; Sharmac, A.; Singhb, M. *Bioorg. Med. Chem. Lett.* **2005**, *15*, 3962.
12. Shah, D. I.; Sharma, M.; Bansal, Y.; Bansal, G.; Singh, M. *Eur. J. Med. Chem.* **1808**, *2008*, 43.
13. Casagrande, C.; Invernizzi, A.; Ferrini, R.; Ferrari, G. G. *J. Med. Chem.* **1968**, *11*, 765.
14. Yu, W. F.; Zhou, Z. M.; Zhu, H. B.; He, L. S. *Chin. J. Org. Chem.* **2006**, *36*, 318.
15. Yu, W. F. Ph.D. Thesis, Beijing Institute of Technology at Beijing, 2004.
16. Yanagisawa, H.; Amemiya, Y.; Kanazaki, T.; Shimoji, Y.; Fujimoto, K.; Kitahara, Y.; Sada, T.; Mizuno, M.; Ikeda, M.; Miyamoto, S.; Furukawa, Y.; Koike, H. *J. Med. Chem.* **1996**, *39*, 323.
17. Cappeli, A.; Nannicini, C.; Gallelli, A. G.; Giuliani, S.; Valenti, G. P.; Mohr, M. A.; Mennuni, L.; Ferrari, F.; Caselli, G.; Giordani, A.; Peris, W.; Makovec, F. *J. Med. Chem.* **2008**, *51*, 2137.
18. David, E. M.; Tonous, N. S.; Michael, K. P. *J. Cardiovasc. Pharmacol.* **2005**, *46*, 585.
19. Yasuhisa, K.; Keiji, K.; Eiko, I.; Takeo, W.; Yoshiyuki, I.; Takehiko, N. *J. Med. Chem.* **1996**, *39*, 5228.
20. Cappeli, A.; Mohr, G. P.; Giuliani, G.; Galeazzi, S.; Anzini, M.; Mennuni, L.; Ferrari, F.; Makovec, F.; Kleinrath, E. M.; Langer, T.; Valoti, M.; Giorgi, G.; Vomero, S. *J. Med. Chem.* **2006**, *49*, 6451.
21. Discovery Studio, 2.0 Version. Accelrys, 2005.
22. Ismail, M. A. H.; Barker, S.; Abou El Ella, D. A.; Abouzid, K. A. M.; Toubar, R. A.; Todd, M. H. *J. Med. Chem.* **2006**, *49*, 1526.
23. Wang, H. Y.; Li, L. L.; Cao, Z. X.; Luo, S. D.; Wei, Y. Q.; Yang, S. Y. *Chem. Biol. Drug Des.* **2009**, *73*, 115.
24. Krovat, E. M.; Langer, T. *J. Med. Chem.* **2003**, *46*, 716.
25. Tuccinardi, T.; Calderone, V.; Rapposelli, S.; Martinelli, A. *J. Med. Chem.* **2006**, *49*, 4305.
26. Gough, K. M.; Belohorová, K.; Kaiser, K. *Sci. Total Environ.* **1994**, *142*, 179.
27. Raul, H. A.; Violeta, Y. M. C.; Sandra, P. M.; Francisco, J. F.; Cesar, A. F. S.; Victor, B.; Hiram, I. B.; Luis, S. Z. R. *Green Chem.* **2010**, *1036*, 12.
28. Sanderson, H.; Thomsen, M. *Toxicol Lett.* **2009**, *187*, 84.
29. Robertson, M. J.; Cunoosamy, M. P.; Clark, K. L. *Br. J. Pharmacol.* **1992**, *106*, 166.
30. Schild, H. O. *Br. J. Pharmacol.* **1947**, *2*, 189.
31. Kubo, K.; Inada, Y. Y.; Kohara, Sugiura, Y.; Ojima, M.; Itoh, K.; Furukawa, Y.; Nishikawa, K.; Naka, T. *J. Med. Chem.* **1993**, *36*, 1772.
32. Kaur, N.; Kaur, A.; Bansal, Y.; Shah, D. I.; Bansal, G.; Singh, M. *Bioorg. Med. Chem.* **2008**, *16*, 10210.